Alqalam Journal of Medical and Applied Sciences. 2025;8(2):896-906
https://doi.org/10.54361/ajmas.258253

Original article

Prediction of Cone Penetration Test Data from Standard Penetration Test Attributes using Support Vector Regression Neural Networks

Dafalla Wadi[1]*, Abuzar Fuad[2], Husam Eldin Ahmed[3], Wenbing Wu[4]

[1]*Department of Engineering Geology, College of Petroleum Geology and Minerals, University of Bahri, P.O. Box 2469, Khartoum, Sudan*
[2]*Department of Chemistry and Earth Science, College of Arts & Sciences, Qatar University, P.O. Box 2713, Doha, Qatar*
[3]*Sea Ports Corporation, Engineering Tests Lab, Port Sudan, Sudan*
[4]*Engineering Research Center of Rock-Soil Drilling Excavation and Protection, Ministry of Education, China University of Geosciences, Wuhan, Hubei 430074, China*
Corresponding Email. wadiadam@cug.edu.cn

Abstract
Although the cone penetration test (CPT) is essential for geotechnical design, it is often not economically feasible and time-consuming to perform the tests at all sites. This work used data from Port Sudan City to create a model to predict CPT values from Standard Penetration Test (SPT) attributes using a Support Vector Regression (SVR) algorithm. This approach converted the SPT into attribute combinations through a stepwise regression analysis. Subsequently, the attributes were converted to CPT by training the SVR neural network with the available CPT data. Cross-validation was performed to assess the credibility of the SPT parameters in the CPT transformation. In this procedure, a quarter of the data set is omitted from the training set each time, and the transformation is recalculated. Next, the accuracy of the transformation in estimating CPT from the deleted data is evaluated; this procedure is applied to all data in the training set. The results show that comparing the actual and predicted CPT gives a good agreement, as indicated by high correlation coefficient values for the training and test data sets. This approach can be used for automated estimation of CPT from SPT parameters and can serve as an extension of conventional techniques.
Keywords. CPT, SPT, Prediction, Artificial Neural Networks, Support Vector Regression, Port Sudan

Introduction

The standard penetration test (SPT) and the cone penetration test (CPT) are the main in situ tests used to characterize the properties of soils in geotechnical engineering practice [1- 4]. Recently, the applications and use of these in-situ tests have steadily increased [5]. SPT is considered a simple, easy approach for underground investigation [6–8], and one of the most frequently used tests in geotechnical research [9 – 13]. SPT is very popular because the correlations between its blow counts, N-value, and soil properties are recognized [14–19], and many specific geotechnical design parameters of the soil are related to the SPT [9, 10].

The CPT was developed in the 1950s at the Dutch Laboratory for Soil Mechanics. Since then, the test has been gaining popularity increasingly as an in-situ test for site exploration and geotechnical design [10,13,20,21]. The CPT results are more accurate than SPT and can give additional information (e.g., pore water pressure) [20-23]. However, it is a high capital investment; a physical soil sample is generally not collected, requires a skilled operator, and is unsuitable for gravel or boulder deposits [24].

It is essential to correlate the static cone tip resistance, qc, of CPT to the blow number, N-value, of SPT so that the accessible database can be effectively utilized. In this context, decades ago, numerous researchers, e.g. [5,25–33], have developed empirical relations between the SPT N-values and CPT cone bearing resistances, qc, for different soil types. Many scholars, e.g., [34-45], have introduced artificial intelligence (AI) to several geotechnical engineering problems and produced successful results. This paper aims to exploit the efficiency of the support vector regression (SVR) algorithm to predict cone penetration prediction results using SPT attributes. SVR embodies the structural risk minimization principle (SRM), which is superior to the conventional neural networks' traditional empirical risk minimization principle (ERM). Despite the widespread acceptance of using mathematical models to predict various geotechnical parameters, no work has been done in our study area. In this paper, we employ a technique using 4-fold cross-validation to evaluate the prediction accuracy of the SVR model outputs.

Geology

The central lithological units along the Sudanese coastal plain of the Red Sea are Tertiary and Mesozoic sediments, overlying the basement rocks. Figure 1 shows the geology of the study area. The raised beach formation consists of marine and continental sediments and reef limestone of Pleistocene and Recent age. These sediments overlie the Tertiary formation [46,47]. Limestone exists at depths exceeding 30 m. The carbonate mineralogy of these limestones reflects a coral origin, as deduced from the balance between the organic and terrigenous carbonate [48,49]. The coastal plain comprises alluvial terrain deposits such as fans of Pleistocene debris. The alluvial deposits consist of marine sediments, clastic materials, reef sand, coral, and shell fragments. The sand of recent age is commonly coarse and arkosic, associated with various

Received*: 03-03-2025 -* ***Accepted****: 04-05-2025 -* ***Published****: 19-05-2025*

gravels; these sands show lateral gradation from unsorted screes, stratified and current-bedded sands, and more rounded gravels. A thin layer of unconsolidated sediments overlays all these units.

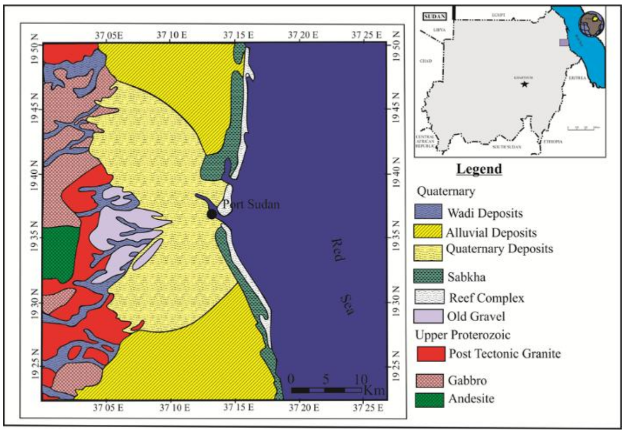

Figure 1. Geological map of the study area (Modified after [50])

Methods

Description of the Dataset

This study used two datasets to develop the proposed SVM Regression model. These data sets, named CPT and SPT parameters (effective overburden pressure, friction angle, and pore water pressure), represent large dimensional data having numerical attribute values. More than 700 SPT-CPT pairs collected at Port Sudan city, Sudan, represent different lithologies that vary from sand, sandy silt, and silty sand soils. The maximum distance between CPT and SPT boreholes is 5 m. The maximum depths of the SPT-CPT boreholes vary from 15 to 34.5 m (Table 1). The reading interval for both SPT and CPT is 1.5 m. Figure 2 shows the measurement of the sites' locations. The water table was encountered in all SPT boreholes at depths ranging between 0.9 and 2.3 m below the existing ground level. The Unified Soil Classification System (USCS) was adapted to classify the collected samples of the SPT sampler. Figure 3 shows typical profiles of the borehole log, standard penetration test's blow count (SPT-N), and cone penetration test's tip resistance (CPT-qc) at the borehole site (BH01).

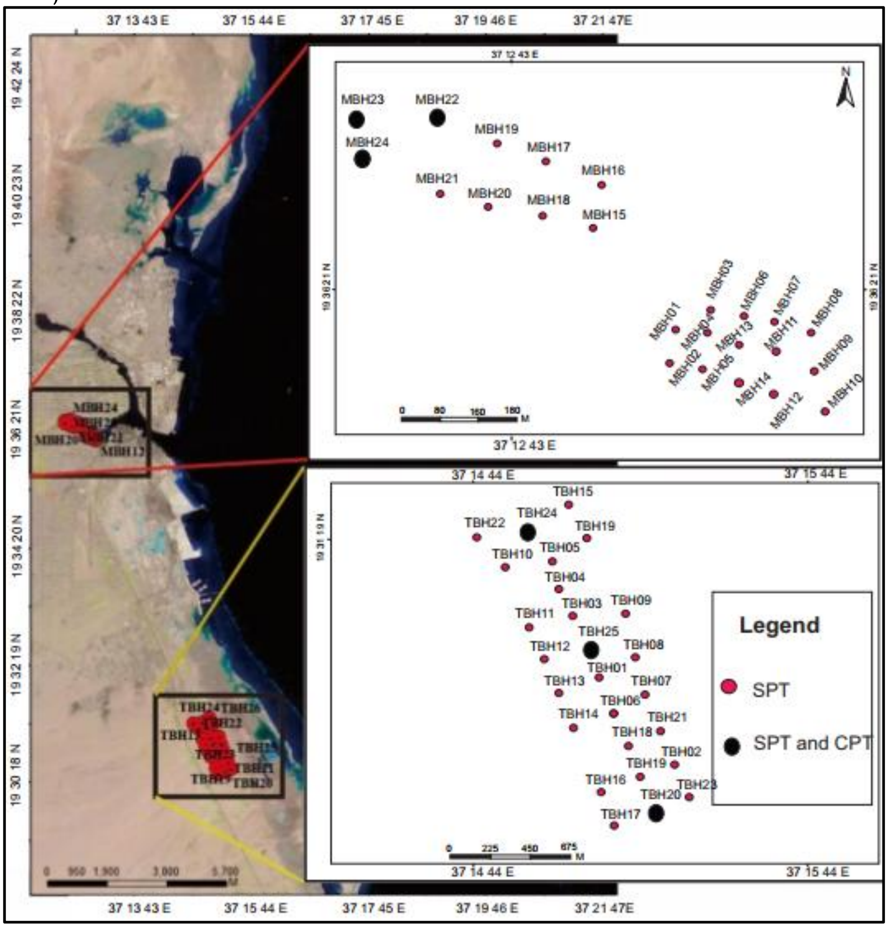

Figure 2. Measurement sites along the Red Sea coastal plain

***Received**: 03-03-2025 - **Accepted**: 04-05-2025 - **Published**: 19-05-2025*

Table 1. Descriptive statistics of the generated database for this study.

Variable	Number	Min	Max	Mean	Std. deviation
Friction angle (FA)	712	27.3	49.5	36.5	4.5
Water pressure (WP)	712	14.7	338.4	132.4	82.0
Effective pressure (EP)	712	13.7	317.0	124.0	76.9
CPT	712	1	30	12.7	6.1
Depth	712	1.5	34.5	13.4	8.3

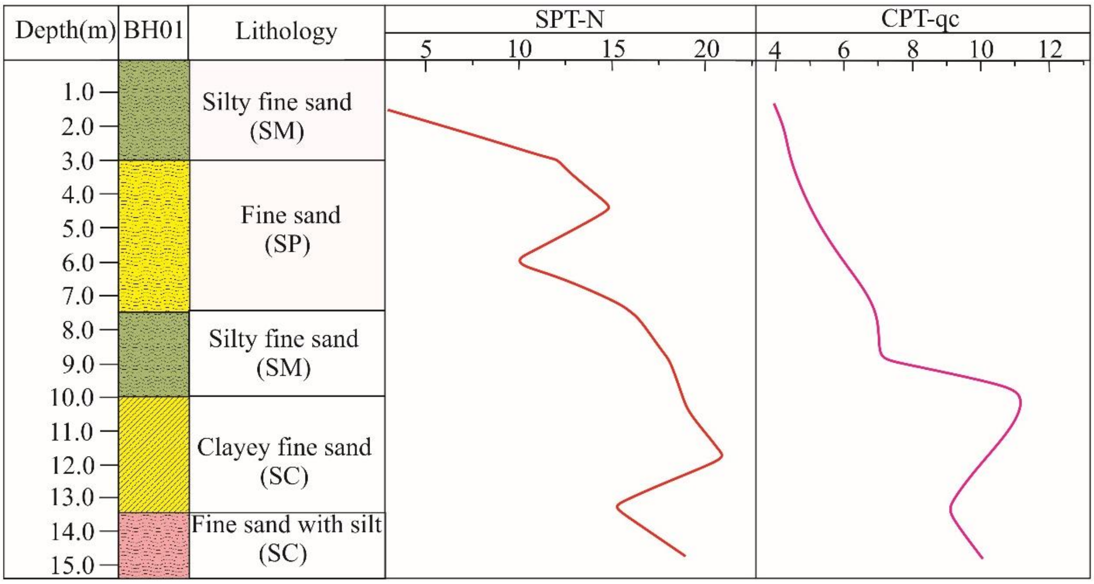

Figure 3. Typical profiles of borehole log, SPT-N, and CPT-qc

Calculating SPT Attributes

This study uses soil type and water table depth to estimate the shear parameters (internal effective overburden pressure, friction angle, and pore water pressure) from the SPT results. Numerous graphs and equations are currently in use to correlate SPT-N with the friction angle (∅) and effective overburden pressure [6, 51 - 53]. Equation 1 is used to estimate the friction angle from SPT-N, which is derived by [54] based on a graph presented by [52] as follows:

$$\emptyset = 27.1 + 0.3N - 0.00054N^2 \qquad (1)$$

Where N represents the SPT-N value.

[29] adapted a study presented by [55] to propose an equation that can be used to calculate effective overburden pressure (σ') from SPT-N and the friction angle (∅) as follows:

$$\emptyset = tan^{-1}\left\{ N \Big/ \left[12.2 + 20.3(\sigma'/P_a)\right] \right\}^{0.34} \qquad (2)$$

Where pa is the atmospheric pressure, equal to 100 kilopascals (kPa).

Water pressure at a test point in saturated media can be estimated relative to atmospheric pressure by a formula proposed by Wood (2014):

$$WP = \gamma_w d \qquad (3)$$

Where WP is the saturated pore water pressure (KPa), γ_w is the unit weight of water, and it is equal to 9.81 kN/m3 [56], and d is the depth of the test (m) below the water table.

Determining the Best Combination of Attributes by Stepwise Regression

A stepwise regression algorithm was proposed by [57] as a fast, although not optimal, approach. The idea behind this approach is the observation that if a linear combination of N attributes is known to optimize some objective function, then the best linear combination of N+1 attributes, including the former N attributes, could only perform equally or better. Here in our work, we employed a backward stepwise regression (Fig. 4), let's assume the model with all potential variables is:

$$Y = \beta_0 + \beta_1 X_1 + \cdots + \beta_{r-1} X_{r-1} + \varepsilon \qquad (4)$$

Where Y is an observer, X_1, X_{r-1} are predictors, β_0 intercept and ε is the error term.

The backward elimination procedure can be applied as follows:

In the first step, let's assume the initial model as above; then, the following r-1 tests are carried out,

$$H_{0j}: \beta_j = 0, \qquad (5)$$

$$j = 1,2, \ldots, r-1$$

Received: 03-03-2025 - **Accepted**: 04-05-2025 - **Published**: 19-05-2025

The lowest partial F-test value F_i corresponding to $H_{0i}: \beta_0 = 0$ or t-test value t_i is compared with the preselected significance values F_0 and t_0 one of two possible steps can be taken.
The first possibility is that if $F_i < F_0$ or $t_i < t_0$ then X_i can be removed, and the new original model is:

$$Y = \beta_0 + \beta_1 X_1 + \cdots + \beta_{l-1} X_{l-1} + \beta_{l+1} X_{l+1} + \cdots + \beta_{r-1} X_{r-1} + \varepsilon \quad (6)$$

The second possibility is that if $F_i > F_0$ or $t_i > t_0$ then the original model is the model we should choose. A detailed mathematical formulation can be found in [58].

Support Vector Regression Algorithm

The support vector regression implements machine learning theory based on classification algorithms, namely, support vector machines. This algorithm, introduced by [59], has been successfully adapted to various problems in science and engineering. Here, we only present a very brief mathematical background of this algorithm; more detailed descriptions can be found in [60, 61].
In any regression model, the objective is to estimate an unknown continuous-parameter function from a finite number set of noisy data $(x_i, y_i), (i = 1, \ldots, n)$, where d-dimensional input $x \in R^d$ and the output $y \in R$. Suppose the statistical model for giving data has the following formulation:

$$y = r(x) + \delta \quad (7)$$

Where $r(x)$ is an unknown target function (regression), and δ is error has zero mean and unit variance σ^2 [62, 63].
In SVM regression, the input $\mathbf{x}$ is first recorded into a m-dimensional feature space via some nonlinear (fixed) mapping, and then a linear model is built in this feature space [63 - 66]. Using mathematical symbolization, the linear model (in the feature space) $f(\mathbf{x}, \omega)$ is given by:

$$f(x, \omega) = \sum_{j=1}^{m} \omega_j g_j(x) + b \quad (8)$$

where $g_j(x), j = 1, \ldots, m$ denotes a set of nonlinear transformations; b is the "bias" term.
Often, the data are assumed to have a zero mean, so the bias term in (2) can be neglected.
The loss function evaluates the accuracy of estimation $L(y, f(x, \omega))$. SVM regression uses a new type of loss function called ε-insensitive loss function proposed by [64]:

$$L_\varepsilon(y, f(x, \omega)) = \begin{cases} 0 & if\ |y - f(x, \omega)| \le \omega \\ |y - f(x, \omega)| - \varepsilon & otherwise \end{cases} \quad (9)$$

The empirical risk is:

$$R_{emp}(\omega) = \frac{1}{n} \sum_{i=1}^{n} L_\varepsilon\left(y_i, f(x_i, \omega)\right) \quad (10)$$

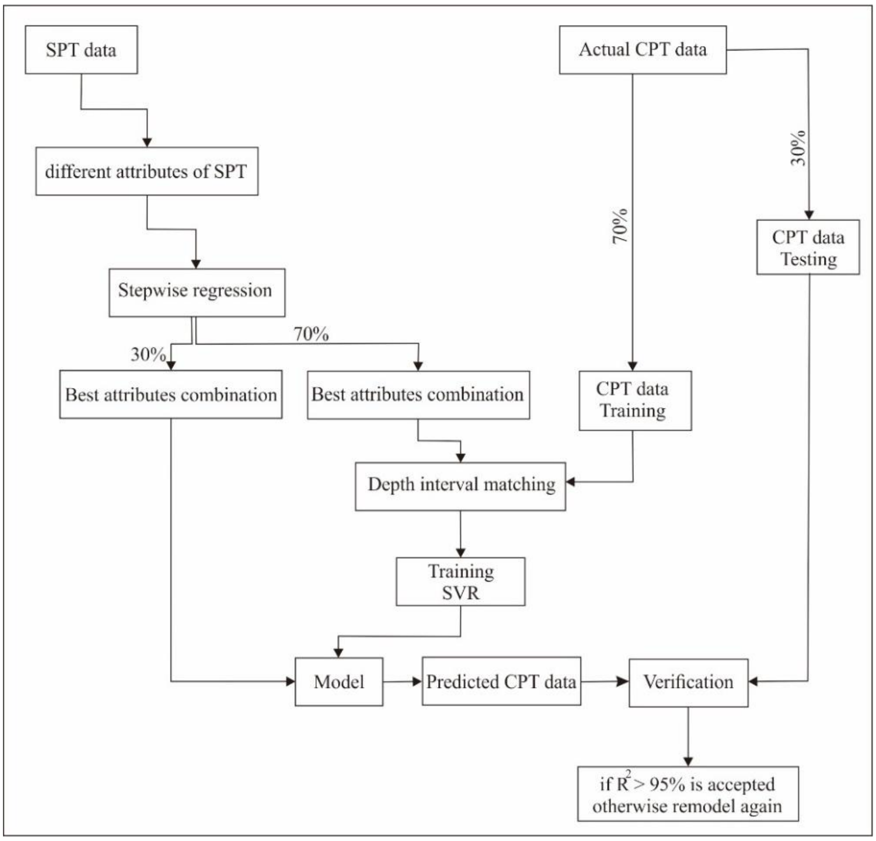

Figure 4. Flowchart of the methodology used in this study

Received: 03-03-2025 - **Accepted**: 04-05-2025 - **Published**: 19-05-2025 https://doi.org/10.54361/ajmas.258253

It can be seen that $\mathcal{E}$-insensitive loss coincides with least-modulus loss and with a particular case of Huber's robust loss function (Vapnik 1999; Vapnik 2013) when $\mathcal{E}= 0$. Hence, we shall compare the prediction practice of SVM (with the proposed chosen $\mathcal{E}$) with regression approximates achieved using least-modulus loss ($\mathcal{E}= 0$) for various noise densities.
SVM regression accomplishes linear regression in a high-dimensional feature space using $\mathcal{E}$-insensitive loss and, at the same time, tries to reduce model complexity by minimizing$\|\omega\|^2$. This can be described by introducing (non-negative) slack variables ξ_i, ξ_i^* $i = 1, \dots, n$, to measure the deviation of training samples outside $\mathcal{E}$-insensitive zone. Thus, SVM regression is formulated as the minimization of the action of the following functional:

$$min\ \frac{1}{2}\|\omega\|^2 + C\sum_{i=1}^{n}(\xi_i + \xi_i^*) \quad (11)$$

$$s.t.\ \begin{cases} y_i - f(x_i,\omega) \le \varepsilon + \xi_i^* \\ f(x_i,\omega) - y_i \le \varepsilon + \xi_i \\ \xi_i, \xi_i^* \ge 0, i = 1, \dots, n \end{cases}$$

This optimization issue can be transformed into a dual problem (Vapnik 1999; Vapnik 2013), and its solution is given by

$$f(x) = \sum_{i=1}^{n_{sv}}(\alpha_i - \alpha_i^*)K(x_i, x) \quad (12)$$

$$s.t.\ 0 \le \alpha_i^* \le C, \qquad 0 \le \alpha_i \le C$$

where $n_{sv}$is the number of Support Vectors (SVs) and the kernel function:

$$K(x, x_i) = \sum_{j=1}^{m} g_j\,(x)g_j(x_i) \quad (13)$$

It is widely known that SVM generalization performance (estimation accuracy) depends on a proper set of meta-parameters, C, $\mathcal{E}$ and the kernel parameters.

Results and discussion

The dataset used in this study comprises 712 points of standard penetration test (SPT) and cone penetration test (CPT). This dataset is interesting because, for each SPT well, there is a CPT well located less than five meters apart. Each SPT N-value was converted to five different attributes. Only three were accepted, and the others were rejected using stepwise regression analysis. Table 1 outlines the descriptive statistical distribution of variables and input parameters used for generating models.
The dataset is partitioned into training and test sets using four validation scenarios. In each scene, 30% of the data will be removed from the practice and kept for testing. Then, repetitions are used for each quarter in each trial. The test set ensures that our model outcomes are reliable and can be generalized to make predictions about new data.
Figures 5 and 6 present a graph and cross-plot of training results for CPT derived with the SVR model of the first validation scenario, respectively. The differences between the actual and predicted CPT values are minimal for all training and test data, supported by a small mean square error and a correlation coefficient almost equal to one (Table 2).

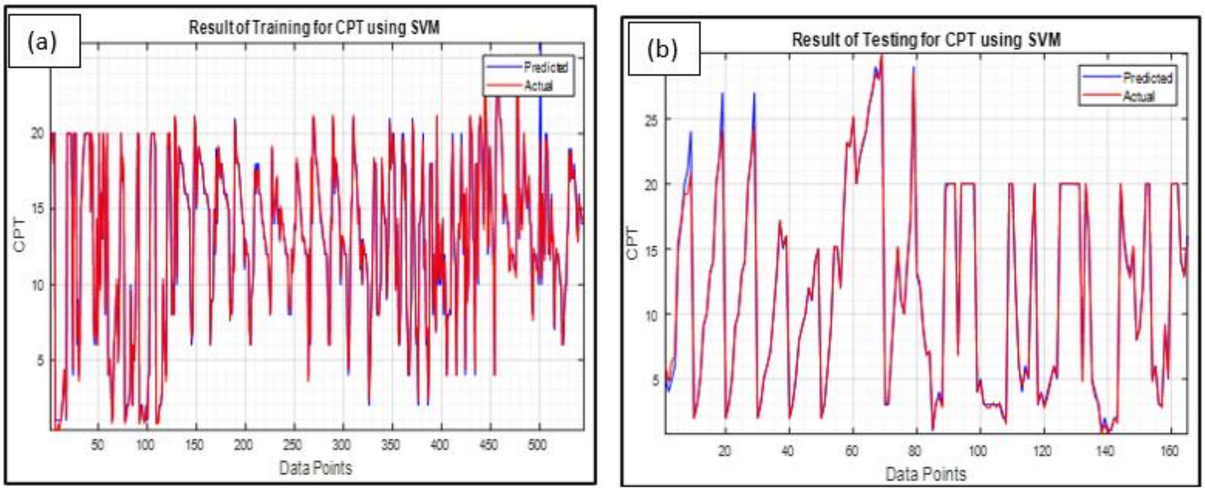

Figure 5. Graph of support vector regression model predicted performance in comparison with actual data of the first quarter of the data set (a), the training set (545 inputs–output data), and (b) the Testing set (165 inputs–output data), first validation scenario

***Received**: 03-03-2025 - **Accepted**: 04-05-2025 - **Published**: 19-05-2025*

https://doi.org/10.54361/ajmas.258253

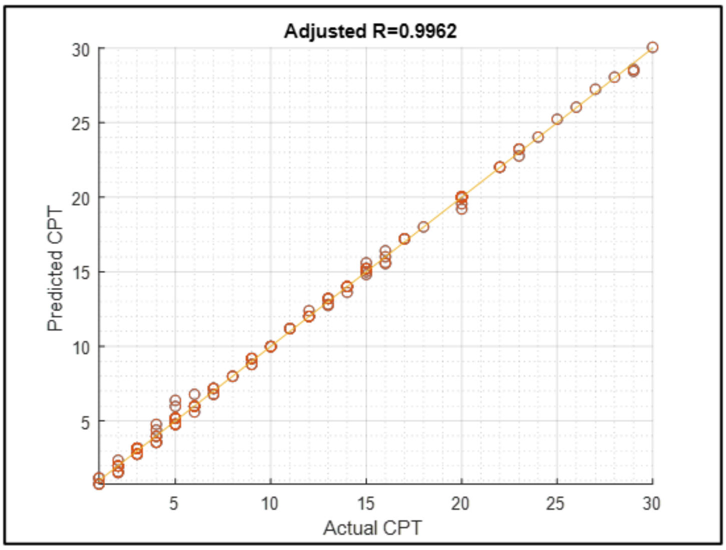

Figure 6. Comparison between the measured and predicted CPT from the SVM regression analysis for the first validation scenario.

Table 2. Performance of SVR models for the training and testing of the four different validation scenarios

Validation	Training RMSE	Testing RMSE	Training R Squared	Testing R Squared
First Quarter	0.53321	0.49118	0.9908	0.9962
Second Quarter	0.57659	0.28729	0.9901	0.9986
Third Quarter	0.57607	0.29870	0.9927	0.9940
Fourth Quarter	0.36559	0.77995	0.9969	0.9749

The second, third, and fourth validation scenario results were employed to ensure the credibility and performance of the suggested SVR models for estimating CPT values from SPT parameters. Figures 7, 8, 9, 10, 11, and 12 present a graph and cross-plot of model outputs and actual CPT.

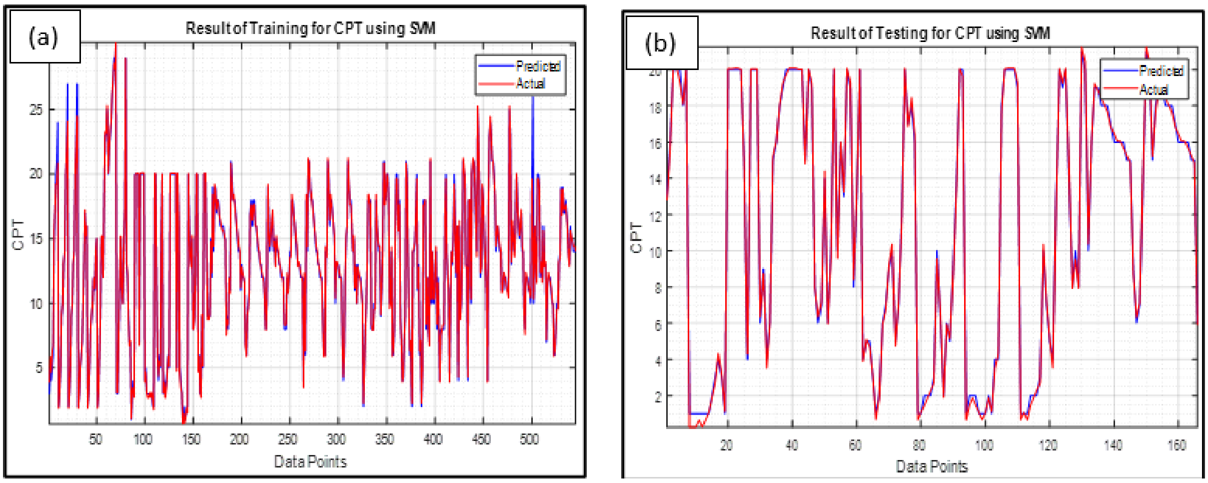

Figure 7. Graph of support vector regression model predicted performance in comparison with actual data of the second quarter of the data set(a), the training set (545 inputs–output data), and (b) the Testing set (165 inputs–output data), second validation scenario.

***Received**: 03-03-2025 - **Accepted**: 04-05-2025 - **Published**: 19-05-2025*

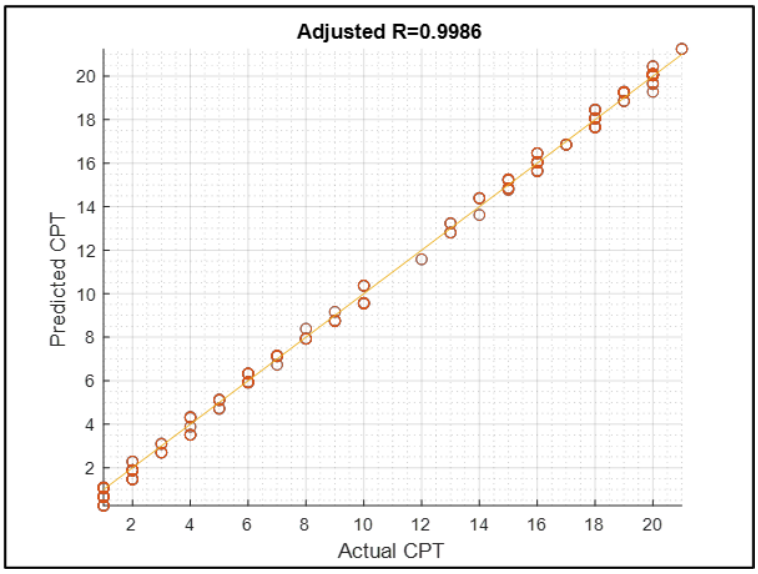

Figure 8. Comparison between the measured and predicted CPT from the SVM regression analysis for the second validation scenario.

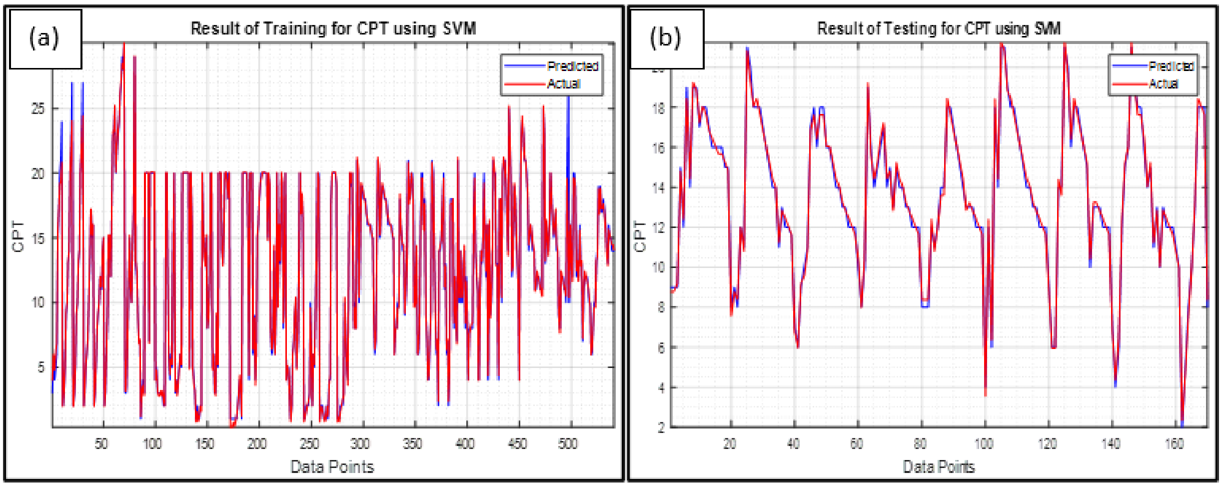

Figure 9. Graph of support vector regression model predicted performance in comparison with actual data of the third quarter of the data set(a), the training set (540 inputs–output data), and (b) the Testing set (170 inputs–output data), third validation scenario.

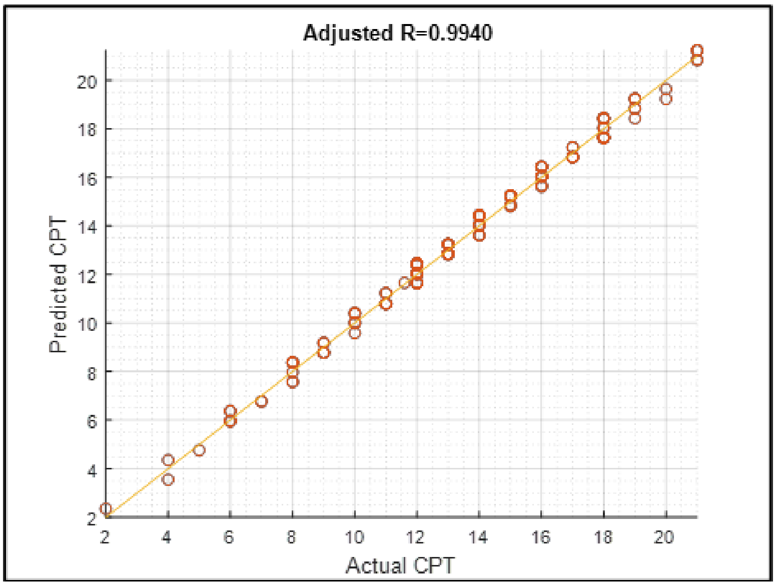

Figure 10. Comparison between the measured and predicted CPT from the SVM regression analysis for the third validation scenario.

***Received**: 03-03-2025 - **Accepted**: 04-05-2025 - **Published**: 19-05-2025*

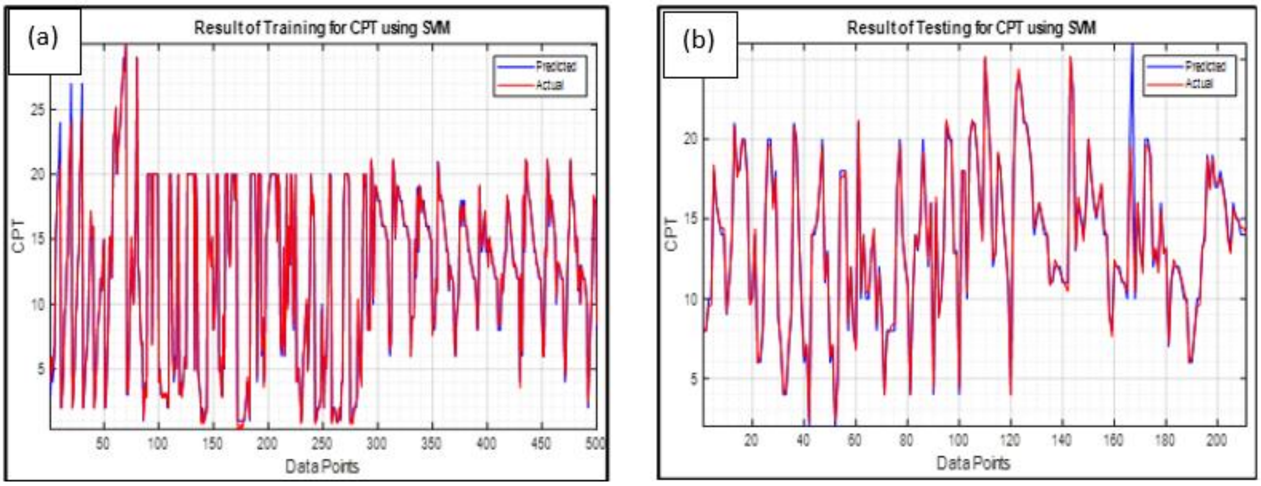

Figure 11. Graph of support vector regression model predicted performance in comparison with actual data of the fourth quarter of the data set (a), the training set (500 inputs–output data), and (b) the Testing set (200 inputs–output data), fourth validation scenario

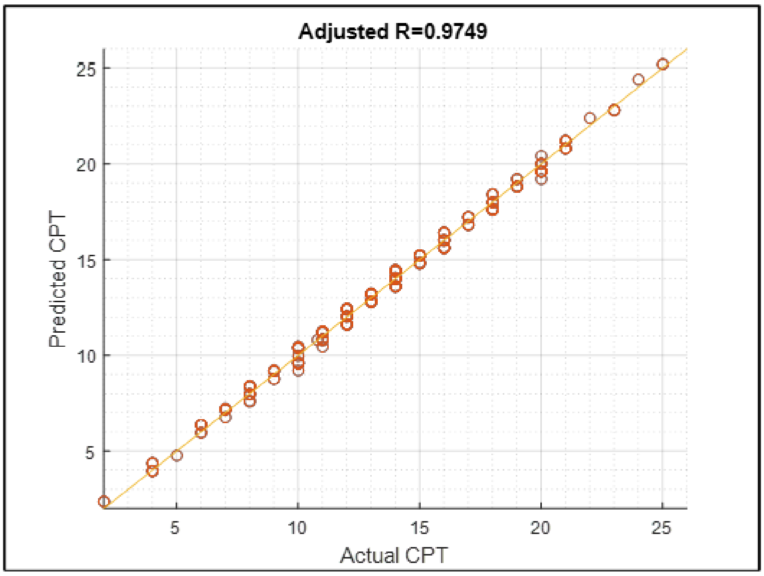

Figure 12. Comparison between the measured and predicted CPT from the SVM regression analysis for the fourth validation scenario.

From previous figures, one can notice that almost the same comparison between the training and actual CPT values produced by the models with a correlation coefficient close to 1 and small mean squared error varies between 0.2 -0.7 and 0.3 – 0.5 for training and testing respectively which can be neglected comparing with our minimum reading of CPT which is equal to 1. Overall, the models produced by the four different validation scenarios show a high capability to produce extreme mean and max CPT readings with high accuracy; this can be noticed from all the figures above.

Figure 13 compares the actual CPT QC value and the SVR-predicted CPT data with depth for the selected six wells. The figures indicate a strong match between the Predicted (Red curve) and actual (black curve) CPT. The location of these six wells is indicated in Figure 2 by black dots.

***Received**: 03-03-2025 - **Accepted**: 04-05-2025 - **Published**: 19-05-2025*

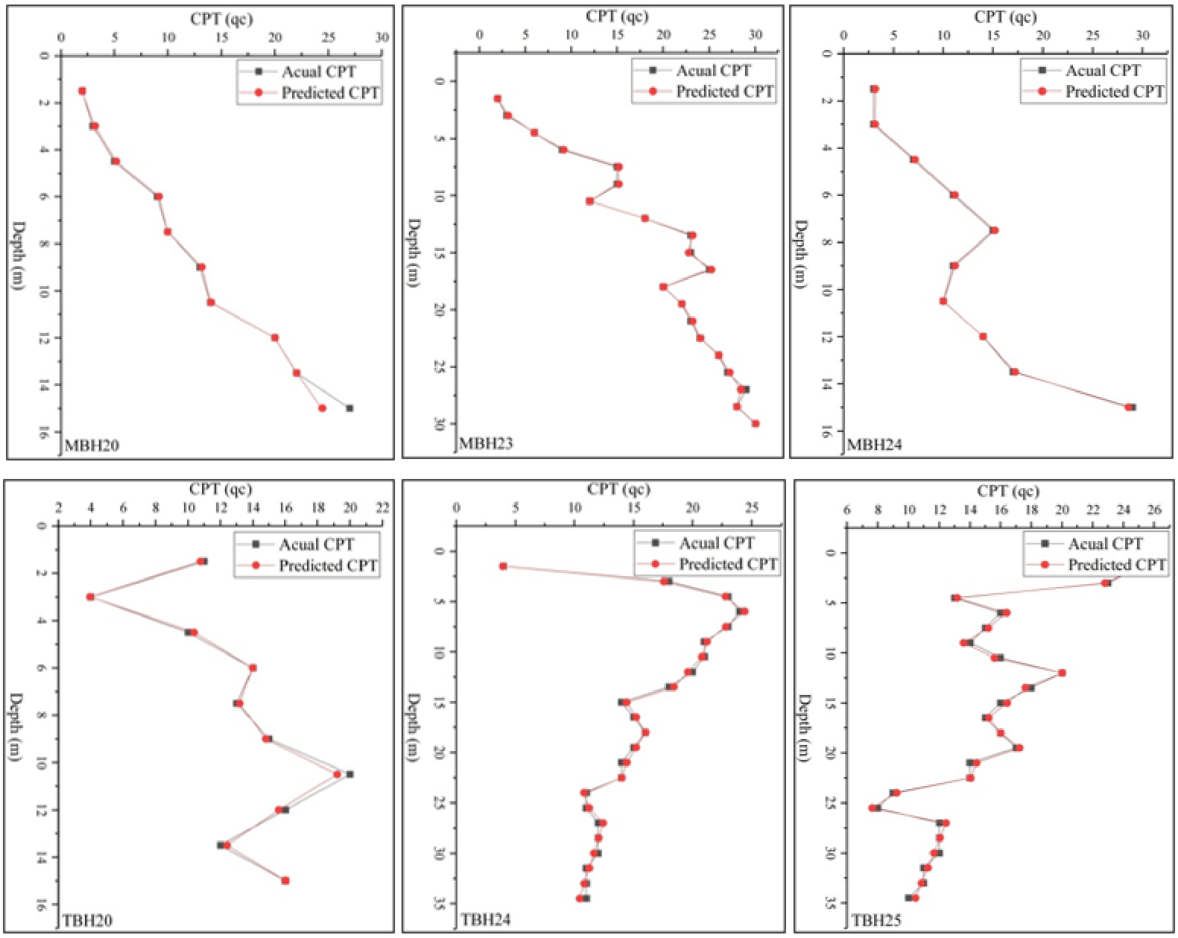

Figure 13. Comparison of CPT qc value with depth from actual CPT data and SVR predicted data

Conclusion

The present work assessed CPT and SPT data from two different geological zones of the southern part of Port-Sudan City, Sudan. The cone penetration test was defined as a standard penetration resistance mathematical function that employed neural network approaches. Using four different validation scenarios, we have exploited the advantage of standard penetration test parameters as inputs of the support vector regression neural networks to estimate cone penetration tests. The experimental results show that the models produced under different validation scenarios match predicted and actual CPT with high accuracy in the assessment. Besides, the models show an excellent capacity to estimate not only common CPT values in the area but also the high and low extreme readings of the CPT. Although the results presented herein are promising, more data from another zone in the area are needed to generalize and improve the accuracy of the studied models.

Acknowledgments

We would like to thank the Sea Ports Corporation of Port Sudan City, Sudan, for providing the data. In addition, China University of Geosciences (Wuhan) is thanked for making the working environment available.

Conflicts of Interest

Declarations of interest: none.

References

1. Seed HB, Tokimatsu K, Harder LF, Chung RM. Influence of SPT procedures in soil liquefaction resistance evaluations. J Geotech Eng. 1985;111(12):1425-1445. doi:10.1061/(ASCE)0733-9410(1985)111:12(1425)
2. Mayne PW, Christopher BR, DeJong J. Manual on subsurface investigations. Nat Highway Inst Sp Pub. 2001;FHWA NHI-01-031.
3. Oh S, Sun CG. Combined analysis of electrical resistivity and geotechnical SPT blow counts for the safety assessment of a fill dam. Environ Geol. 2008;54(1):31. doi:10.1007/s00254-007-0790-y
4. Tarawneh B. Predicting standard penetration test N-value from cone penetration test data using artificial neural networks. Geosci Front. 2017;8(1):199-204. doi:10.1016/j.gsf.2016.02.003
5. dos Santos MD, Bicalho KV. Proposals of SPT-CPT and DPL-CPT correlations for sandy soils in Brazil. J Rock Mech Geotech Eng. 2017;9(6):1152-1158. doi:10.1016/j.jrmge.2017.08.001

***Received**: 03-03-2025 - **Accepted**: 04-05-2025 - **Published**: 19-05-2025*

6. Gibbs HJ. Research on determining the density of sands by spoon penetration testing. In: Proc 4th Int Conf SMFE. 1957;1:35-39.
7. Lacroix Y, Horn HM. Direct determination and indirect evaluation of relative density and its use on earthwork construction projects. In: Evaluation of Relative Density and its Role in Geotechnical Projects Involving Cohesionless Soils. ASTM International; 1973.
8. Skempton AW. Standard penetration test procedures and the effects in sands of overburden pressure, relative density, particle size, ageing, and overconsolidation. Geotechnique. 1986;36(3):425-447. doi:10.1680/geot.1986.36.3.425
9. Decourt L. The standard penetration test, state-of-the-art report. Proc 12th ICSMFE. 1989;4:2405-2416.
10. Akca N. Correlation of SPT-CPT data from the United Arab Emirates. Eng Geol. 2003;67(3-4):219-231. doi:10.1016/S0013-7952(02)00181-3
11. Sivrikaya O, Toğrol E. Determination of undrained strength of fine-grained soils by means of SPT and its application in Turkey. Eng Geol. 2006;86(1):52-69. doi:10.1061/(ASCE)1090-0241(1998)124:5(389)
12. Kayabaşı A. Some empirical equations for predicting standard penetration test blow counts in clayey soils: a case study in Mersin, Turkey. Arab J Geosci. 2015;8(9):7643-7654. doi:10.1007/s12517-014-1694-2
13. Aral IF, Gunes E. Correlation of Standard and Cone Penetration Tests: Case Study from Tekirdag (Turkey). IOP Conf Ser Mater Sci Eng. 2017;245:032028. doi:10.1088/1757-899X/245/3/032028
14. Skempton AW. The colloidal activity of clays. Sel Pap Soil Mech. 1953:106-118.
15. Seed HB, Woodward RJ, Lundgren R. Fundamental aspects of the Atterberg limits. J Soil Mech Found Div. 1966;92(Closure). doi:10.1061/JSFEAQ.0000685
16. Imai T, Yoshimura Y. Elastic wave velocity and soil properties in soft soil. Tsuchito-Kiso. 1970;18(1):17-22.
17. Imai T. Correlation of N-value with S-wave velocity and shear modulus. Proc 2nd Eur Symp Penetration Test. 1982.
18. Nath SK, Thingbaijam KKS. Assessment of seismic site conditions: a case study from Guwahati city, Northeast India. Pure Appl Geophys. 2011;168(10):1645-1668.
19. Sun CG, Cho CS, Son M, Shin JS. Correlations between shear wave velocity and in-situ penetration test results for Korean soil deposits. Pure Appl Geophys. 2013;170(3):271-281. doi:10.1007/s00024-012-0516-2
20. Robertson PK. Soil classification using the cone penetration test. Can Geotech J. 1990;27(1):151-158.
21. Sargand SM, Masada T, Abdalla B. Evaluation of cone penetration test-based settlement prediction methods for shallow foundations on cohesionless soils at highway bridge construction sites. J Geotech Geoenviron Eng. 2003;129(10):900-908.
22. De Beer EE. Bearing capacity and settlement of shallow foundation on sand. Proc Symp Duke Univ. 1965:15-34.
23. Meyerhof GG. Shallow foundations. J Soil Mech Found Div. 1965;91(Proc Paper 4275).
24. Robertson PK, Wride CE. Evaluating cyclic liquefaction potential using the cone penetration test. Can Geotech J. 1998;35(3):442-459. doi:10.1139/t98-017
25. Meigh AC, Nixon IK. Comparison of in situ tests for granular soils. Proc 5th Int Conf Soil Mech Found Eng. 1961;1:499-507.
26. Schmertmann JH. Static cone to compute static settlement over sand. J Soil Mech Found Div. 1970. doi:10.1061/JSFEAQ.0001418
27. Robertson PK, Campanella RG. Interpretation of cone penetration tests. Part I: Sand. Can Geotech J. 1983;20(4):718-733.
28. Ismael NF, Jeragh AM. Static cone tests and settlement of calcareous desert sands. Can Geotech J. 1986;23(3):297-303. doi:10.1139/t86-043
29. Kulhawy FH, Mayne PW. Manual on estimating soil properties for foundation design. *EPRI-EL-6800.* 1990.
30. Danziger BR, Velloso DA. Correlations between the CPT and the SPT for some Brazilian soils. Proc Int Symp Cone Penetration Test. 1995:155-159.
31. Czado B, Pietras JS. Comparison of the cone penetration resistance obtained in static and dynamic field tests. AGH J Min Geoeng. 2012;36(1):97-105.
32. Souza JMS, Danziger BR, Danziger FAB. The influence of the relative density of sands in SPT and CPT correlations. Soils Rocks. 2012;35(1).
33. Shahri AA, Juhlin C, Malemir A. A reliable correlation of SPT-CPT data for the southwest of Sweden. Electron J Geotech Eng. 2014;19(1013):e1032.
34. Zhou Y, Wu X. Use of neural networks in the analysis and interpretation of site investigation data. Comput Geotech. 1994;16(2):105-122. doi:10.1016/0266-352X(94)90017-5
35. Goh ATC. Empirical design in geotechnics using neural networks. Geotechnique. 1995;45(4):709-714. doi:10.1680/geot.1995.45.4.709
36. Toll DG. Artificial intelligence applications in geotechnical engineering. Electron J Geotech Eng. 1996;1:767-773.
37. Shi J, Ortigao JAR, Bai J. Modular neural networks for predicting settlements during tunneling. J Geotech Geoenviron Eng. 1998;124(5):389-395.
38. Shahin MA, Jaksa MB, Maier HR. Artificial neural network applications in geotechnical engineering. Aust Geomech. 2001;36(1):49-62.
39. Shahin MA, Jaksa MB, Maier HR. Applications of Artificial Neural Networks in Foundation Engineering. Aust Geomech. 2003.
40. Bendana R, del Cano A, Pilar de la Cruz M. Contractor selection: fuzzy-control approach. Can J Civ Eng. 2008;35(5):473-486. doi:10.1139/L07-127
41. Nejad FP, Jaksa MB, Kakhi M, McCabe BA. Prediction of pile settlement using artificial neural networks based on standard penetration test data. Comput Geotech. 2009;36(7):1125-1133.

***Received**: 03-03-2025 - **Accepted**: 04-05-2025 - **Published**: 19-05-2025*

42. Elshorbagy A, Corzo G, Srinivasulu S, Solomatine DP. Experimental investigation of the predictive capabilities of data-driven modeling techniques in hydrology- Part 1: Concepts and methodology. Hydrol Earth Syst Sci. 2010;14(10):1931-1941. doi:10.5194/hess-14-1931-2010
43. Gholamnejad J, Bahaaddini H, Rastegar M. Prediction of the deformation modulus of rock masses using Artificial Neural Networks and Regression methods. J Min Environ. 2013;4(1):35-43. doi:10.22044/jme.2013.144
44. Asci M, Kurtulus C, Kaplanvural I, Mataracioglu MO. Correlation of SPT-CPT Data from the Subsidence Area in Gölcük, Turkey. Soil Mech Found Eng. 2015;51(6):268-272. doi:10.1007/s11204-015-9288-x
45. Moghaddasi MR, Noorian-Bidgoli M. ICA-ANN, ANN, and multiple regression models for the prediction of surface settlement caused by tunneling. Tunn Undergr Space Technol. 2018;79:197-209.
46. Carella R, Scarpa M. Geological results of exploration in Sudan by AGIP Mineraria. 4th Arab Petrol Congr. 1962:23.
47. Berry L, Whiteman AJ, Bell SV. Some radiocarbon dates and their geomorphological significance, the emerged reef complex of the Sudan. Z Geomorphol. 1966;10(2):119-143.
48. Bunter MAG, Magid AA. The Sudanese Red Sea: 1. New developments in stratigraphy and petroleum-geological evolution. J Petrol Geol. 1989;12(2):145-166. doi:10.1111/j.1747-5457.1989.tb00230.x
49. Cowell PJ, Stive MJ, Niedoroda AW, de Vriend HJ, Swift DJ, Kaminsky GM, Capobianco M. The coastal-tract (part 1): a conceptual approach to aggregated modeling of low-order coastal change. J Coast Res. 2003:812-827.
50. Wadi D, Wu W, Fuad A, Ahmed HE, Abdalla R. Correlation between SPT and CPT for Sandy Soils in Port Sudan City using the Linear Regression Model. Afr J Eng Technol. 2022;6(2). doi:10.47959/AJET.2021.1.1.6
51. Meyerhof GG. Penetration tests and bearing capacity of cohesionless soils. J Soil Mech Found Div. 1956;82(1):1-19. doi:10.1061/JSFEAQ.0000001
52. Peck RB, Hanson WE, Thornburn TH. Foundation engineering. Vol 10. Wiley; 1974.
53. Hettiarachchi H, Brown T. Use of SPT blow counts to estimate shear strength properties of soils: energy balance approach. J Geotech Geoenviron Eng. 2009;135(6):830-834. doi:10.1061/(ASCE)GT.1943-5606.0000016
54. Wolff TF. Pile capacity prediction using parameter functions. ASCE Geotech Spec Publ. 1989;23:96-107.
55. Schmertmann JH. Measurement of in situ shear strength, SOA Report. Proc ASCE Spec Conf In Situ Meas Soil Prop. 1975;2:57-138.
56. NCOEF Engineering. Fundamentals of Engineering: Supplied-reference Handbook. Kaplan AEC Engineering; 2003.
57. Draper NR, Smith H. Applied regression analysis. Vol 326. John Wiley & Sons; 2014.
58. Hosmer Jr DW, Lemeshow S, Sturdivant RX. Applied logistic regression. Vol 398. John Wiley & Sons; 2013.
59. Vapnik V, Chervonenkis A. A note on the class of perceptron. Autom Remote Control. 1964;24.
60. Burges CJ. A tutorial on support vector machines for pattern recognition. Data Min Knowl Discov. 1998;2(2):121-167. doi:10.1023/A:1009715923555
61. Shawe-Taylor J, Cristianini N. An introduction to support vector machines and other kernel-based learning methods. Vol 204. Cambridge University Press; 2000.
62. Cherkassky V, Shao X, Mulier FM, Vapnik VN. Model complexity control for regression using VC generalization bounds. IEEE Trans Neural Netw. 1999;10(5):1075-1089. doi:10.1109/72.788648
63. Cherkassky V, Mulier FM. Learning from data: concepts, theory, and methods. John Wiley & Sons; 2007.
64. Vapnik VN. An overview of statistical learning theory. IEEE Trans Neural Netw. 1999;10(5):988-999. doi:10.1109/72.788640
65. Smola AJ, Schölkopf B. A tutorial on support vector regression. Stat Comput. 2004;14(3):199-222. doi:10.1023/B:STCO.0000035301.49549.88
66. Vapnik V. The nature of statistical learning theory. Springer Science & Business Media; 2013.

Received*: 03-03-2025 -* ***Accepted****: 04-05-2025 -* ***Published****: 19-05-2025*